lubricants

MDPI

Article

Wear Characterization of Cemented Carbides (WC–CoNi) Processed by Laser Surface Texturing under Abrasive Machining Conditions

Shiqi Fang [1,2,3], Luis Llanes [1,2,*] and Dirk Bähre [3]

[1] CIEFMA-Departament de Ciència dels Materials i Enginyeria Metal.lúrgica, Universitat Politècnica de Catalunya, EEBE—Campus Diagonal Besòs, Barcelona 08019, Spain; shiqi.fang@upc.edu

[2] Barcelona Research Center in Multiscale Science and Engineering, Universitat Politècnica de Catalunya, Barcelona 08019, Spain

[3] Institute of Production Engineering, Saarland University, Saarbrücken 66123, Germany; d.baehre@mx.uni-saarland.de

* Correspondence: luis.miguel.llanes@upc.edu; Tel.: +34-9-3401-1083

Received: 3 June 2017; Accepted: 19 June 2017; Published: 22 June 2017

Abstract: Cemented carbides are outstanding engineering materials widely used in quite demanding material removal applications. In this study, laser surface texturing is implemented for enhancing, at the surface level, the intrinsic bulk-like tribological performance of these materials. In this regard, hexagonal pyramids patterned on the cutting surface of a tungsten cemented carbide grade (WC–CoNi) have been successfully introduced by means of laser surface texturing. It simulates the surface topography of conventional honing stones for abrasive application. The laser-produced structure has been tested under abrasive machining conditions with full lubrication. Wear of the structure has been characterized and compared, before and after the abrasive machining test, in terms of changes in geometry aspect and surface integrity. It is found that surface roughness of the machined workpiece was improved by the laser-produced structure. Wear characterization shows that laser treatment did not induce any significant damage to the cemented carbide. During the abrasive machining test, the structure exhibited a high wear resistance. Damage features were only discerned at the contacting surface, whereas geometrical shape of pyramids remained unchanged.

Keywords: cemented carbide; laser surface texturing; abrasive machining; wear; surface integrity

1. Introduction

Cemented carbides are forefront engineering materials for extreme industrial applications, such as tools and components used for metal cutting, mining, rock drilling, and metal forming [1–3]. Cemented carbides are composites consisting of a hard phase and a soft one. The former corresponds to ceramic particles, usually tungsten carbide (WC), whereas the latter commonly refers to cobalt (Co) and/or Nickel (Ni) based metallic alloys. It combines the hardness and wear resistance of the carbide grains with the adequate toughness of the metallic binder. On the other hand, considering that many of the applications where those materials are employed involve high contact load demands at the surface, their performance may be enhanced by complementing their bulk-like attributes with surface modification technologies (e.g., [4,5]).

In the early 1990s, ultra-short pulse (10^{-12}–10^{-15} s) laser was introduced as an efficient processing method for surface treatment. Surface treatment using ultra-short pulse laser processing is called laser surface texturing (LST). LST has become popular in the domain of tribology, where it has been continuously attracting deeper attention. In general, LST is used as an advanced strategy to improve

tribological performance of functional surfaces, since it provides modified surfaces shaped with high accuracy and excellent quality [6,7]. Current research validates the view that LST is suitable to machine hard materials, such as cemented carbides and ceramics [8–10]. Different from other non-abrasive shaping routes, such as electrical discharge machining (EDM), common damage induced by thermal-related machining (e.g., [11]) is effectively reduced during LST [12,13]. Accordingly, laser induced patterns on cemented carbide have resulted in satisfactory findings regarding tribological applications, particularly in terms of reducing friction of the contacting surfaces [14,15]. For example, it has been proven that a supporting part made of cemented carbide with laser-produced dimples can effectively reduce friction of the contacting surface in honing-like service condition with full lubrication [16].

In a recent study by the authors, surface topography of a commercial honing stone (cubic boron nitride composite) has been characterized with the purpose of simulating and producing its geometrical features on a WC–CoNi cemented carbide surface using LST [17]. It is the aim of this work to characterize the wear performance of such laser-shaped structure on the cemented carbide, from both a quantitative and a qualitative perspective. In doing so, a brief introduction of structure production and the abrasive machining test is given first. Then, the geometrical properties of the modified surface, i.e. hexagonal pyramids, are measured using laser scanning microscopy (LSM), before and after the abrasive machining test. Surface integrity of pyramids is assessed in cross-sections milled by means of a focused ion beam. It enables analysis of wear mechanisms involved in the abrasive machining tests. The results indicate that LST does not induce any significant defects to the patterns, and that laser-shaped structure is able to maintain its profile and geometrical aspect during the abrasive machining test with full lubrication.

2. Material and Experimental Aspects

2.1. Studied Material and Surface Machined by Laser Surface Texturing (LST)

A cobalt/nickel-based cemented tungsten carbide grade is used as tool material in this work. It contains a binder amount of 28 wt % (Co + Ni). The embedded carbides have an average size of 20 µm. Microstructural characteristics of the selected cemented carbide are shown in Table 1. Figure 1a shows the microstructure of the investigated material, as characterized by Scanning Electron Microscopy (SEM, Zeiss Neon 40, Barcelona, Spain).

Table 1. Microstructural characteristics of the selected cemented tungsten carbide grade (WC–CoNi).

WC-Grain Size (µm)	Co (wt %)	Ni (wt %)	Density (g/cm^3)	Hardness (HV30)
20	14	14	12.82	610

The ultra-short pulse laser (picosecond, HYPER25 Coherent Kaiserslautern GmbH, Kaiserslautern, Germany) integrated in a five-axis micromachining system (GL.5, GFH GmbH) is implemented to modify the functional surface of the cemented carbide. Table 2 illustrates the laser characteristics and LST parameters applied in the experiments.

Table 2. Laser parameters used for the production of dimples.

Laser Type	Laser Source	Pulse Duration (ps)	Wave Length (nm)	Frequency (Hz)	Fluence (J/cm^2)
ps-laser	Nd:YVO4	10	532	200 K	0.5

The used samples have the dimension of 20 × 3 mm^2, and the working surfaces should be fine polished prior to the laser treatment. In the experiment, the laser beam scans the surface at the speed of 1000 mm/s line by line along *X*-axis. A feed of 0.2 µm by layer is applied along the *Z*-axis, and the thickness of 25 µm is then removed. In total, 343 hexagonal pyramids are produced on the sample

surface (Figure 1b). The following parameters are used to describe the pyramid geometrical properties (Figure 1c):

- d_1: interval between two adjacent hexagonal pyramids along the *X*-axis
- d_2: interval between two adjacent hexagonal pyramids along the *Y*-axis
- a_1: bottom side length of the hexagonal pyramid
- a_2: top side length of the hexagonal pyramid
- S_1: surface area of the pyramid bottom
- S_2: surface area of the pyramid top
- h: height the hexagonal pyramid
- α: slope at the measuring position A-A
- β: slope at the measuring position B-B

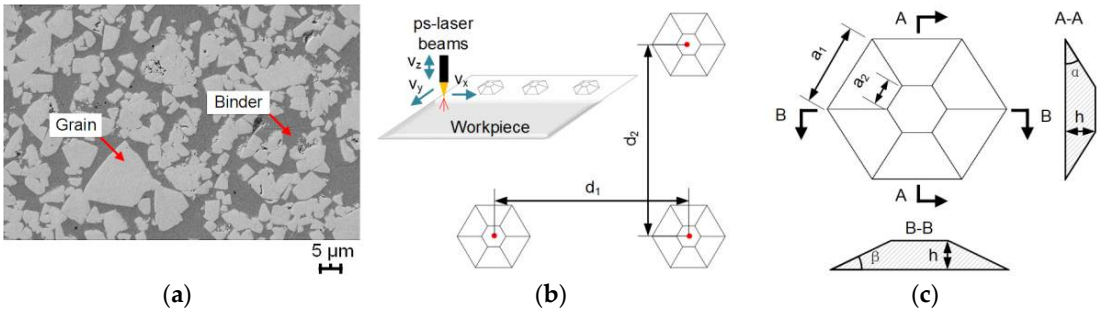

Figure 1. (**a**) Scanning Electron Microscopy (SEM) image of the investigated cemented carbide; (**b**) Schematic illustration of pyramid production using ultra-short pulse laser beams; (**c**) Geometrical design of single hexagonal pyramid.

Five measurements are carried out and Table 3 summarizes the geometrical features of the LST-shaped hexagonal pyramid patterns. High geometrical precision has been achieved in the LST machining processing.

Table 3. Geometrical parameters of the hexagonal pyramid patterns shaped by laser surface texturing (LST).

Parameters	d_1 (µm)	d_2 (µm)	a_1 (µm)	a_2 (µm)	S_1 (µm^2)	S_2 (µm^2)	h (µm)	α (°)	β (°)
Mean	404.5	403.5	63.7	31.1	9.1×10^3	2.3×10^3	21.6	27.1	30.2
Standard Deviation	1.9	1.4	2.5	2.2	0.2	0.3	1.6	0.7	0.8

2.2. Abrasive Machining Test

The abrasive machining test of the laser-shaped hexagonal pyramids have been carried out by means of an in-house test bench, which is constructed on the basis of external honing processes (Figure 2a) [18]. This workbench can characterize the abrasive machining processes by force measurement (Figure 2b). The laser-shaped surface was placed on the force measurement unit with a certain feed against the workpiece. The workpiece is made of common commercial steel and rotates at the speed of 500 rpm, and oscillates at the speed of 1000 mm/min. Meanwhile, the test sample moves with a stepping feed of 2 µm. The used lubricant Kadio50 has a kinematic viscosity v of 5 mm^2/s at the temperature of 40 °C. The flow rate of the lubricant is set to 0.07 Bar. Each test lasts about 42 s and has been repeated 10 times.

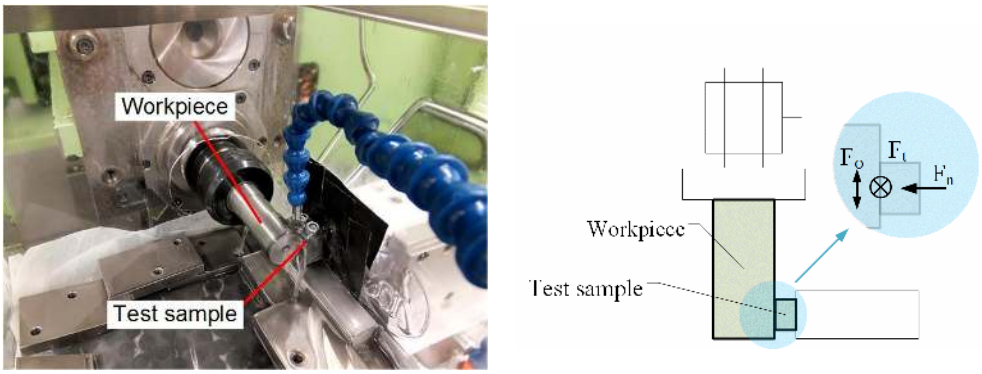

(**a**) (**b**)

Figure 2. (**a**) Workbench for abrasive machining processes; (**b**) dynamics in the abrasive machining process.

3. Results and Remarkable Observations

3.1. Geometrical Properties of the Laser-Shaped Structure

After the tests, the geometrical properties of the hexagonal pyramids have been measured using LSM. The surface coordination obtained by LSM was recorded and exported to reconstruct the 3D model of the hexagonal pyramid. The obtained geometrical properties were compared with the ones before machining (Figure 3a,b). Figure 3c,d illustrates the reconstructed 3D model of a single pyramid before and after testing. The contour lines and the corresponding colors indicate the profiles and the height of the pyramid. The 3D model intuitively proves that the top of the pyramid experienced obvious damage, and the structure was gradually worn out from the top to the bottom. However, the geometrical aspect of the hexagonal pyramid remained unchanged at the bottom.

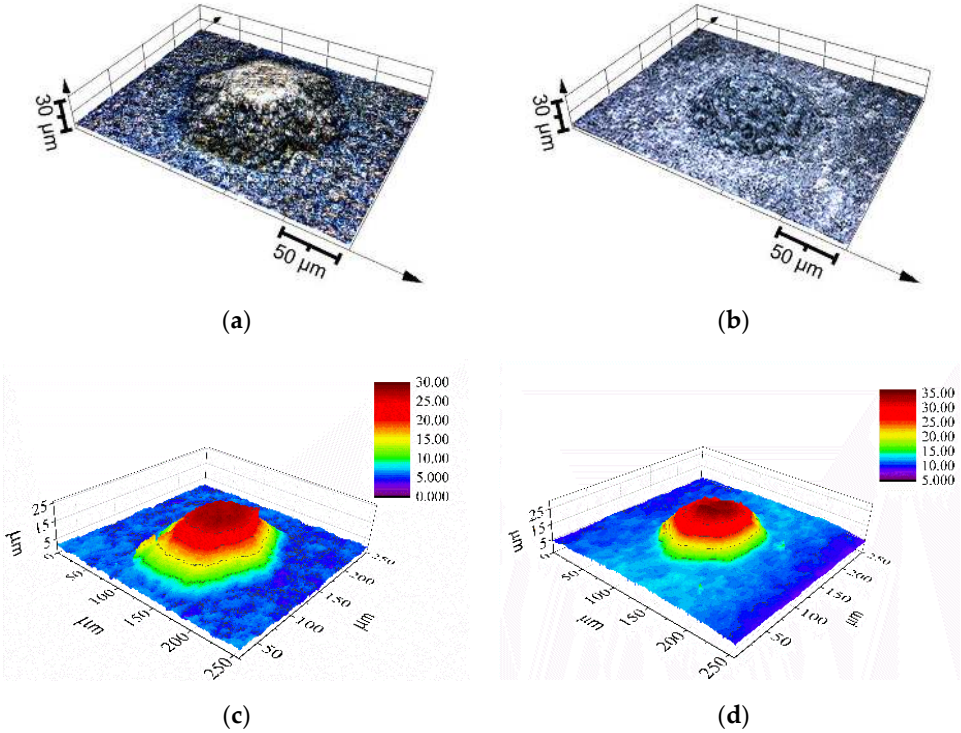

(**a**) (**b**)

(**c**) (**d**)

Figure 3. Hexagonal pyramid 3D characterization using laser scanning microscopy (LSM): (**a**) before testing and (**b**) after testing; 3D model reconstruction using Origin 9.0: (**c**) before testing and (**d**) after testing.

After the tests, five measurements are also carried out and the measurement results of the geometrical features are summarized in Table 4. The average side length a_1 at the top is 61.7 µm, and the one at the bottom a_2 is 28.1 µm. The surface area S_1 at the bottom is 9.1 × 10^3 µm^2 and S_2 at the top is 2.4 × 10^3 µm^2. The height h of the pyramid is 17.7 µm and the slope angles α and β are 24.8° and 27.4°, respectively.

Table 4. Geometrical properties of the hexagonal pyramid patterns after abrasive machining test.

Parameters	a_1 (µm)	a_2 (µm)	S_1 (×10^3 µm^2)	S_2 (×10^3 µm^2)	h (µm)	α (°)	β (°)
Mean	61.7	28.1	9.1	2.4	17.7	24.8	27.4
Standard Deviation	5.0	2.0	1.1	0.5	2.3	4.1	1.1

Figure 4 shows the quantitative comparison of the geometrical properties of the hexagonal pyramids, before and after the tests. It is observed that side lengths a_1 and a_2 are slightly changed (Figure 4a), indicating the slight deformation of the pyramids. Surface areas S_1 and S_2 at the pyramid bottom and top remain approximately constant (Figure 4b), indicating the pyramid shape stays generally unchanged. The slope angles α and β became also slightly smaller, due to the deformation of the pyramids (Figure 4c). The height of the pyramid decreased about 3.9 µm, corresponding to a wear speed of 1.1 × 10^{-3} µm/r, knowing the workpiece had a total rotation of 3500 during the tests (Figure 4d).

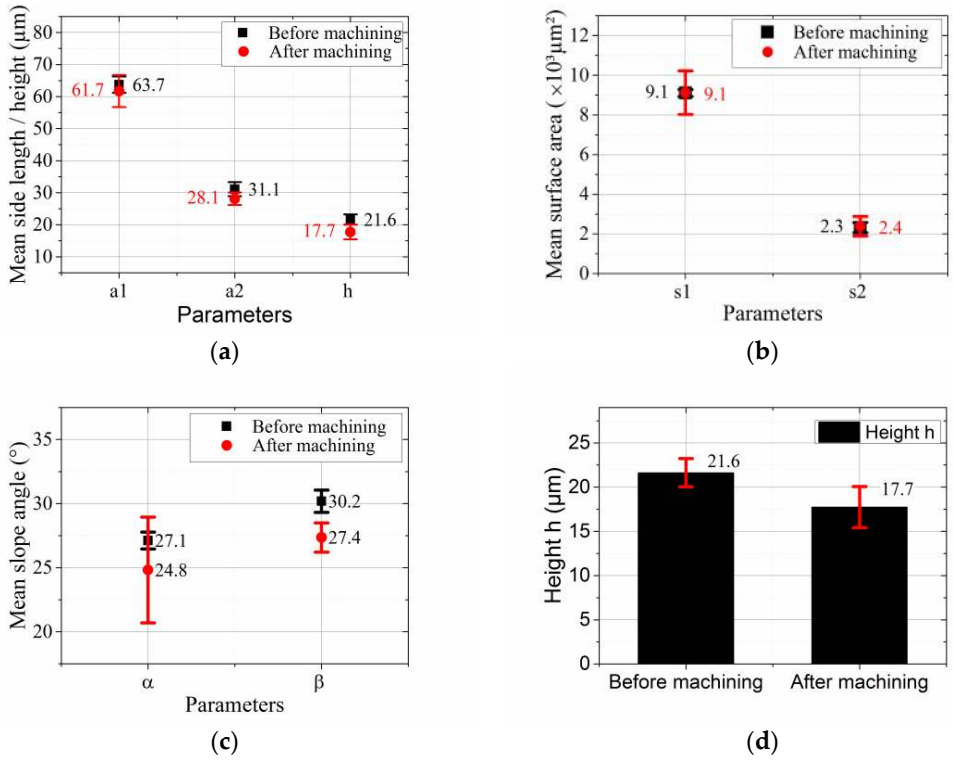

Figure 4. Comparison of the geometrical properties of the hexagonal pyramids before and after machining: (**a**) side lengths and height; (**b**) surface area; (**c**) slope angles; and (**d**) height evolution.

3.2. Surface Integrity Assessment

Figure 5 shows SEM images of the hexagonal pyramid produced by LST: overall appearance, local details, and cross-sectional inspection. The LST-produced structure exhibits an excellent hexagonal and homogenous profile at the top and the bottom, referring to the geometrical design (Figure 5a),

as compared to other conventional machining methods, such as EDM [19]. Surface integrity may be described as satisfactory after the laser treatment (Figure 5b): the binder experiences more ablation than the WC grains, as a consequence of their different melting and vaporization temperatures [20,21]; and stripes, referring to laser-induced periodic surface structures (LIPSSs), are found on the WC grains, due to the interference of the surface-electromagnetic waves [22–24]. Cross-sectional analysis can assess that binder ablation and stripes (interference structures) do not penetrate into the material subsurface (Figure 5c).

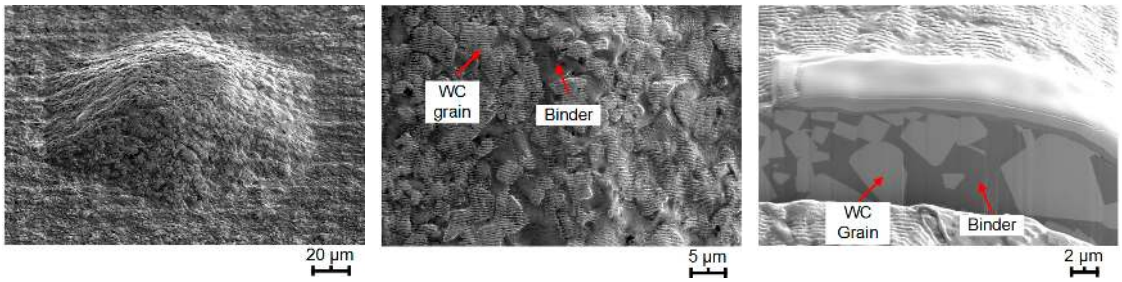

Figure 5. (**a**) Single hexagonal pyramid produced by LST; (**b**) Surface morphology from the top to the bottom (left to right in the image); (**c**) Cross sectional investigation (images taken by SEM).

After the abrasive machining test, surface integrity of the involved hexagonal pyramid has been inspected and assessed as compared to its initial state, in order to evaluate its wear performance during the test. The shape of the pyramid can still be clearly distinguished, but the profile becomes rather blurred at some parts of the slopes; for example, the ones situated opposite the machining direction (Figure 6a). This finding can be explained by the fact that the wear of the workpiece produced by the abrasive processes was stacked there. The disappearance of the stripes at the top surface of the pyramid suggests that the top platform was demolished during the machining processes. The wear of the pyramid began from the top and gradually went deep as a consequence of sliding against the workpiece (Figure 6b). It has also been discerned that the binder was worn out faster than WC grains, due to abrasion and some fissures produced at the grains. However, these damage features were not observed to penetrate and develop into subsequent failure at the subsurface level (Figure 6c). The unchanged shape of the pyramid in the machining process, especially the maintaining of the top platform, is with no doubt favorable to obtaining an effective establishment of a stable lubrication film, therefore, the tribological system can be kept stable.

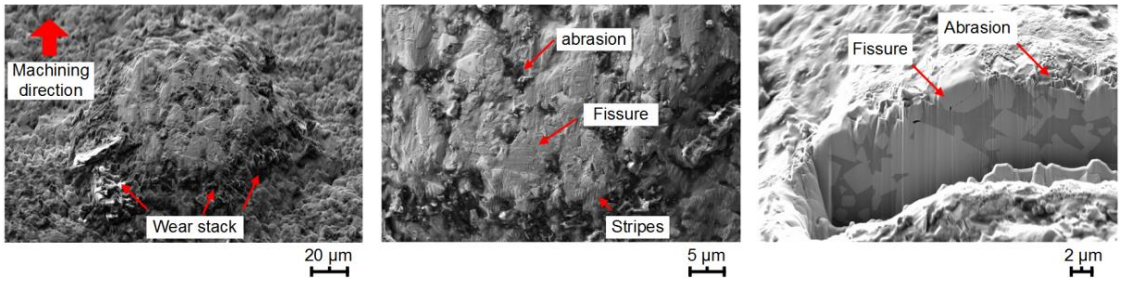

Figure 6. Hexagonal pyramids after abrasive machining test characterized by SEM: (**a**) overall appearance; (**b**) Details of the working surface; (**c**) Cross-sectional inspection.

4. Conclusions and Discussion

In this work, a cemented carbide sample with LST-shaped structure, i.e., hexagonal pyramids, has been tested as a cutting tool on an in-house test bench. The influence of such surface modification

on the corresponding tribological response has been characterized through changes of geometrical properties and surface integrity. It was found that surface structure maintained a hexagonal shape during the abrasive machining test. Such findings signify the wear resistance of the laser-shaped structure against significant rupture, and point out its capability to be used on cutting edges of tools. Wear is mainly found to take place at the top surface of the structure in the form of abrasion for the binder and micro-cracks of the grains. However, such damage features did not go deeper into the subsurface. Meanwhile, it can be assumed that the hexagonal pyramids will be worn out more intensively when testing duration increases or more workpieces are involved. Therefore, these findings imply that additional treatments following LST, such as coating, may be considered to further enhance the wear resistance of LST-processed tools. Furthermore, considering that observed wear around the structure may have negative effects in terms of thermal transmission, lubrication distribution, and/or stress concentration emergence, research efforts on improving the structure geometry are recalled.

Acknowledgments: The work leading to this publication was supported by the German Academic Exchange Service (DAAD) with funds from the German Federal Ministry of Education and Research (BMBF) and the People Program (Marie Curie Actions) of the European Union's Seventh Framework Program (FP7/2007–2013) under REA grant agreement 605728 (P.R.I.M.E.—Postdoctoral Researchers International Mobility Experience). The authors are also grateful for equipment support from Photonik-Zentrum Kaiserslautern e.V., as well as for the material supplying by and Saar-Hartmetall und Werkzeuge GmbH. Finally, this contribution has also been partly funded by the Spanish Ministry of Economy and Competitiveness through grant MAT2015-70780-C4-3P (MINECO/FEDER).

Author Contributions: Shiqi Fang, Luis Llanes and Dirk Bähre conceived and designed the experiments; Shiqi Fang performed the experiments; Shiqi Fang analyzed the data; Dirk Bähre and Luis Llanes contributed reagents/materials/analysis tools; Shiqi Fang and Luis Llanes wrote the paper.

Conflicts of Interest: The authors declare no conflict of interest.

References

1. Exner, H.E. Physical and chemical nature of cemented carbides. *Int. Met. Rev.* **1979**, *24*, 149–173. [CrossRef]
2. Gurland, J. New scientific approaches to development of tool materials. *Int. Mater. Rev.* **1988**, *33*, 151–166. [CrossRef]
3. Egashira, K.; Hosono, S.; Takemoto, S.; Masao, Y. Fabrication and cutting performance of cemented tungsten carbide micro-cutting tools. *Precis. Eng.* **2011**, *35*, 547–553. [CrossRef]
4. Jacobson, S.; Hogmark, S. Surface modifications in tribological contacts. *Wear* **2009**, *266*, 370–378. [CrossRef]
5. Konyashin, I.; Ries, B.; Hlawatschek, S. Engineered surfaces on cemented carbides obtained by tailored sintering techniques. *Surf. Coat. Technol.* **2014**, *258*, 300–309. [CrossRef]
6. Momma, C.; Chichkov, B.N.; Nolte, S.; von Alvensleben, F.; Tünnermann, A.; Welling, H.; Wellegehausen, B. Short-pulse laser ablation of solid targets. *Opt. Commun.* **1996**, *129*, 134–142. [CrossRef]
7. Geiger, M.; Roth, S.; Becker, W. Influence of laser-produced microstructures on the tribological behavior of ceramics. *Surf. Coat. Technol.* **1998**, *100*, 17–22. [CrossRef]
8. Chichkov, B.N.; Momma, C.; Nolte, S.; von Alvensleben, F.; Tünnermann, A. Femtosecond, picosecond and nanosecond laser ablation of solids. *Appl. Phys. A* **1996**, *63*, 109–115. [CrossRef]
9. Li, T.; Lou, Q.; Dong, J.; Wei, Y.; Liu, J. Phase transformation during surface ablation of cobalt-cemented tungsten carbide with pulsed UV laser. *Appl. Phys. A* **2001**, *73*, 391–397. [CrossRef]
10. Dumitru, G.; Romano, V.; Weber, H.P.; Sentis, M.; Marine, W. Femtosecond ablation of ultrahard materials. *Appl. Phys. A* **2002**, *74*, 729–739. [CrossRef]
11. Llanes, L.; Martinez, E.; Idañez, E.; Casas, B.; Esteve, J. Infuence of electrical discharge machining on the sliding contact response of cemented carbides. *Int. J. Refract. Met. Hard Mater.* **2001**, *19*, 35–40. [CrossRef]
12. M'Saoubi, R.; Outeiro, J.C.; Chandrasekaran, H.; Dillon, O.W., Jr.; Jawahir, I.S. A review of surface integrity in machining and its impact on functional performance and life of machined products. *Int. J. Sustain. Manuf.* **2008**, *1*, 203–236. [CrossRef]
13. Fatima, A.; Whitehead, D.J.; Mativenga, P.T. Femtosecond laser surface structuring of carbide tooling for modifying contact phenomena. *Proc. Inst. Mech. Eng. B* **2016**, *230*, 3–18. [CrossRef]

14. Dumitru, G.; Romano, V.; Weber, H.P.; Haefke, H.; Gerbig, Y.; Pflüger, E. Laser microstructuring of steel surfaces for tribological applications. *Appl. Phys. A* **2000**, *70*, 485–487. [CrossRef]
15. Geiger, M.; Popp, U.; Engel, U. Excimer laser micro texturing of cold forging tool surfaces—Influence on tool life. *CIRP Ann. Manuf. Technol.* **2002**, *51*, 231–234. [CrossRef]
16. Fang, S.; Herrmann, T.; Rosenkranz, A.; Gachot, C.; Marro, F.G.; Mücklich, F.; Llanes, L.; Bähre, D. Tribological performance of laser patterned cemented tungsten carbide parts. *Procedia CIRP* **2016**, *42*, 439–443. [CrossRef]
17. Fang, S.; Llanes, L.; Engstler, M.; Baehre, D.; Soldera, F.; Muecklich, F. Surface topography quantification of super hard abrasive tools by laser scanning microscopy. *Mater. Perform. Charact.* **2016**, *5*, 796–815. [CrossRef]
18. Bähre, D.; Fang, S.Q.; Gliche, J.; Trapp, K. Set-up of a test bench for the investigation of single parameter effects in abrasive processes by force measurements. *Adv. Mater. Res.* **2014**, *1052*, 441–446. [CrossRef]
19. Llanes, L.; Casas, B.; Idanez, E.; Marsal, M.; Anglada, M. Surface integrity effects on the fracture resistance of electrical-discharge-machined WC-Co cemented carbides. *J. Am. Ceram. Soc.* **2004**, *87*, 1687–1693. [CrossRef]
20. Yao, Y.L.; Chen, H.; Zhang, W. Time scale effects in laser material removal: A review. *Int. J. Adv. Manuf. Technol.* **2005**, *26*, 598–608. [CrossRef]
21. Li, T.; Lou, Q.; Dong, J.; Wei, Y.; Liu, J. Selective removal of cobalt binder in surface ablation of tungsten carbide hardmetal with pulsed UV laser. *Surf. Coat. Technol.* **2001**, *145*, 16–23. [CrossRef]
22. Bonse, J.; Krüger, J.; Höhm, S.; Rosenfeld, A. Femtosecond laser-induced periodic surface structures. *J. Laser Appl.* **2012**, *24*, 42006. [CrossRef]
23. Bonse, J.; Rosenfeld, A.; Krüger, J. On the role of surface plasmon polaritons in the formation of laser-induced periodic surface structures upon irradiation of silicon by femtosecond-laser pulses. *J. Appl. Phys.* **2009**, *106*, 104910. [CrossRef]
24. Okamuro, K.; Hashida, M.; Miyasaka, Y.; Ikuta, Y.; Tokita, S.; Sakabe, S. Laser fluence dependence of periodic grating structures formed on metal surfaces under femtosecond laser pulse irradiation. *Phys. Rev. B* **2010**, *82*, 1–5. [CrossRef]